Contraction and AICAR Stimulate IL-6 Vesicle Depletion From Skeletal Muscle Fibers In Vivo

Hans P.M.M. Lauritzen,[1] Josef Brandauer,[2] Peter Schjerling,[3] Ho-Jin Koh,[1] Jonas T. Treebak,[4] Michael F. Hirshman,[1] Henrik Galbo,[5] and Laurie J. Goodyear[1]

Recent studies suggest that interleukin 6 (IL-6) is released from contracting skeletal muscles; however, the cellular origin, secretion kinetics, and signaling mechanisms regulating IL-6 secretion are unknown. To address these questions, we developed imaging methodology to study IL-6 in fixed mouse muscle fibers and in live animals in vivo. Using confocal imaging to visualize endogenous IL-6 protein in fixed muscle fibers, we found IL-6 in small vesicle structures distributed throughout the fibers under basal (resting) conditions. To determine the kinetics of IL-6 secretion, intact quadriceps muscles were transfected with enhanced green fluorescent protein (EGFP)-tagged IL-6 (IL-6-EGFP), and 5 days later anesthetized mice were imaged before and after muscle contractions in situ. Contractions decreased IL-6-EGFP–containing vesicles and protein by 62% ($P < 0.05$), occurring rapidly and progressively over 25 min of contraction. However, contraction-mediated IL-6-EGFP reduction was normal in muscle-specific AMP-activated protein kinase (AMPK) α2-inactive transgenic mice. In contrast, the AMPK activator AICAR decreased IL-6-EGFP vesicles, an effect that was inhibited in the transgenic mice. In conclusion, resting skeletal muscles contain IL-6–positive vesicles that are expressed throughout myofibers. Contractions stimulate the rapid reduction of IL-6 in myofibers, occurring through an AMPKα2-independent mechanism. This novel imaging methodology clearly establishes IL-6 as a contraction-stimulated myokine and can be used to characterize the secretion kinetics of other putative myokines. ***Diabetes*** **62:3081–3092, 2013**

Skeletal muscle is a critical tissue for whole-body glucose metabolism during both normal and pathological conditions. There is increasing evidence that skeletal muscles express myokines, hormone-like factors that are released into the serum to function in an autocrine, paracrine, or endocrine manner (1–5). In recent years, numerous myokines have been proposed to be secreted from muscle, including interleukin-6 (IL-6) (1), fibroblast growth factor 21 (3), follistatin-like 1 (2), insulin-like 6 factor (4), and most recently irisin (5). Thus, skeletal muscle is potentially the largest endocrine organ in the body, and myokine release may provide a significant mechanism for crosstalk with other tissues.

Of these putative myokines, IL-6 has been the most extensively studied (1,6). IL-6 has been proposed to be secreted from skeletal muscle and to function in an autocrine manner to activate signaling proteins mediating glucose uptake (7), glycogen metabolism (8), fat metabolism (9), and muscle hypertrophy (10). Despite considerable investigation of IL-6, the exact cellular origin of IL-6 within the muscle tissue is not well understood. In fact, previous studies have not clearly detected IL-6 protein within the muscle fibers from human biopsies (11) or mouse muscle sections (10) unless a state of inflammation (12,13) or injury (10) was present. It is possible that the biopsy procedure itself causes IL-6 release and contamination from invading macrophages (14), interfering with the ability to determine the exact level and localization of IL-6 within the muscle fibers. Thus, whether IL-6 is present in skeletal muscle fibers under normal, resting conditions is not fully understood.

There is considerable evidence that exercise increases circulating concentrations of IL-6 based on studies demonstrating an increased arterial/venous IL-6 difference across contracting skeletal muscles (1,6,15–17). However, studies analyzing the cellular localization of IL-6 within muscle fibers during exercise are limited. In one study, bicycle ergometer exercise for 2 h resulted in increased detection of IL-6 protein near the sarcolemma region of vastus lateralis muscle (11). Since light microscopy cannot distinguish the sarcolemma from the interstitial space, one interpretation of this finding is that the detected IL-6 did not originate from muscle fibers but instead arose from biopsy- and/or exercise-induced macrophage infiltration (14). If muscle fibers are the source of increased circulating IL-6 during exercise, then the number of secretory vesicles containing IL-6 in the muscle fibers might be expected to decrease with contractions, not increase. Given the ambiguities of previous data, one aim of the current study was to determine the kinetics and time course of a putative IL-6 release from contracting skeletal muscle fibers.

Exercise increases AMP-activated protein kinase (AMPK) activity in skeletal muscle, and AMPK signaling pathways have been proposed to mediate multiple metabolic effects (18). Exercise-stimulated AMPK activity in muscle has been associated with an increase in circulating IL-6 during exercise (19), although a direct link between AMPK activation and IL-6 protein release from muscle fibers has not been reported (19,20). AMPK stimulation has also been reported to alter IL-6 expression, albeit with conflicting results (21–23). In one report, 24 h of incubation of C2C12 muscle cells with the AMPK activator AICAR increased IL-6 mRNA (21). In another report, 2–4 h of AICAR incubation of soleus and extensor digitorum longus muscles decreased IL-6 mRNA

From the [1]Research Division, Joslin Diabetes Center and Harvard Medical School, Boston, Massachusetts; the [2]Department of Health Sciences, Gettysburg College, Gettysburg, Pennsylvania; the [3]Department of Orthopedic Surgery M, Institute of Sports Medicine, Bispebjerg Hospital and Center for Healthy Aging, Faculty of Health Sciences, University of Copenhagen, Copenhagen, Denmark; [4]The Novo Nordisk Foundation Center for Basic Metabolic Research, Faculty of Health Sciences, University of Copenhagen, Copenhagen, Denmark; and the [5]Department of Rheumatology and Institute of Inflammation Research, Rigshospitalet, Copenhagen University Hospital, Copenhagen, Denmark.

Corresponding author: Laurie J. Goodyear, laurie.goodyear@joslin.harvard.edu.

Received 12 September 2012 and accepted 8 June 2013.

DOI: 10.2337/db12-1261

H.P.M.M.L. and J.B. contributed equally to the study.

(22,23) and IL-6 secretion into the incubation media (23). Thus, the role of AMPK in the regulation of IL-6 in skeletal muscle has not been established.

In the current study, we determined if intact muscle fibers express IL-6 under basal, resting conditions. In addition, we determined if muscle contraction and AICAR regulate IL-6 secretion in vivo. Finally, we investigated the potential role of AMPKα2 in contraction-stimulated IL-6 release. To address these questions, we developed novel imaging techniques that allow for kinetic analysis of IL-6–containing vesicles within intact muscle fibers in vivo. These studies establish that IL-6 is a contraction-induced myokine in intact muscle fibers, but that AMPKα2 activity does not mediate contraction-stimulated IL-6 secretion.

RESEARCH DESIGN AND METHODS

Protocols for animal use were in accordance with the guidelines of the Institutional Animal Care and Use Committee of the Joslin Diabetes Center and the National Institutes of Health. All animals were housed in a 12:12-h light:dark cycle and fed a standard laboratory chow and water ad libitum. Whole-body IL-6 knockout (B6.129S2-Il6^{tm1kopf}/J) and corresponding wild-type (C57BL/6J) mice were obtained from The Jackson Laboratory. Wild-type NMRI (Naval Medical Research Institute) mice were obtained from Taconic, Denmark. AMPKα2-inactive transgenic mice on an FVB background and matched controls were also studied (24).

In situ contraction. Animals underwent a 12-h fast and were anesthetized with 90 mg/kg pentobarbital. Sciatic nerves were bilaterally isolated, and electrodes were placed around each nerve, which were connected to a Grass S88 stimulation unit. One tibialis anterior (TA) muscle was stimulated for 45 min (1 train/sec, 500-ms train duration, 100 Hz, 0.1-ms pulse duration, 1–13 V), while the muscle of the contralateral leg served as the control experiment. After the conclusion of the contraction protocol, TA muscles were removed and immediately fixed as previously described (25).

Image analysis of endogenous IL-6 localization in muscle fibers. From the fixed TA muscles single fibers were isolated. Thirty fibers from each muscle were arbitrarily isolated from the muscle with fine forceps and were subjected to immunostaining as previously described (25,26). Primary antibodies against IL-6 (ab-6672) and Golgi marker 130 (GM130 [ab-40881]) were obtained from Abcam (Cambridge, MA). The secondary Alexa488 antibody (#A11008) was obtained from Molecular Probes (Eugene, OR). Confocal images were obtained blindly on a Zeiss LSM-410 confocal microscope with Argon Krypton 488-nm laser line for excitation of Alexa488. Z stacks were collected using a 63× Apochromat (1.4 NA) Zeiss oil immersion objective and a zoom of 2. Z stacks were collected at every third muscle fiber (n = 8 out of the 30 fibers arbitrarily isolated) at two different intracellular locations. The distance covered 6 μm from the interior (approximately 12 μm from the surface) toward the surface of the fiber using 8× frame image averaging.

Plasmid procedures and transfection. The plasmid "IL-6-pEGFP C-fusion" was generated by PCR amplification of the IL-6 coding region from a mouse full-length EST clone (BC132458, IMAGE #40130735; Source BioScience, Nottingham, U.K.) using the following primers: 5′-GCG GAA TTC GTC AAT TCC AGA AAC CGC TA-3′and 5′-CGC CTC GAG GGT TTG CCG AGT AGA TCT CAA AGT-3′. This PCR product was cut with *Eco*RI and *Xho*I and inserted in the *Eco*RI and *Bam*HI sites of pEGFP-N1 (Clontech Laboratories, Inc., Mountain View, CA). To enable ligation between the *Xho*I site and the *Bam*HI site, a linker was added, which was made by hybridization between the two oligonucleotides 5′-TCGACGGATATCCGCGGGCCCGG-3′and 5′-GATCCCG-GGCCCGCGGATATCCG-3′. This three fragment cloning produced a coding sequence fusion of IL-6 to the N-terminus of enhanced green fluorescent protein (EGFP). The inserted sequence was confirmed by sequencing. The Golgi marker pEYFP (enhanced yellow fluorescent protein)-Golgi was used as a nonsecreted control and was obtained from Clontech (#6909–1). DNA was grown in *E. coli* TOP10 cells and extracted using a Plasmid Mega Kit (Qiagen, Valencia, CA). DNA was dissolved in water.

For intravital imaging experiments, the quadriceps muscles of 7- to 9-week-old male ICR mice (Taconic, Derwood, MD) were anesthetized, the skin covering the quadriceps was opened, and the superficial muscle fibers were transfected with gene gun bombardment with 1 μg IL-6-EGFP or EYFP-Golgi cDNA/0.5 mg gold, as previously described (26,27). After transfection, the skin was closed with sutures and the animals recovered for 5 days.

Intravital imaging. Five days after transfection, the overnight fasted mice were anesthetized with phenobarbital sodium (90 mg/kg, intraperitoneally), and the skin covering the quadriceps muscle was opened to expose the quadriceps. The mice were mounted on their side in dental cement, as previously described (27,28). In the animals used for contraction-stimulation experiments, microeletrodes were placed in the groin and knee region of the quadriceps muscle, just before applying a coverglass. In the animals used for AICAR- or caffeine-stimulation experiments, a catheter was placed in a tail vein. Ten minutes after mounting, a confocal image was recorded just beneath the surface (~3 μm below the sarcolemma) of the transfected muscle fiber. Another image 6 μm deeper inside the fiber was also recorded. There was an additional 30-min temperature and movement stabilization period and another basal pair of images were obtained and used as t = 0 (t denotes accumulated contraction time) throughout the study. The images obtained just after mounting and 30 min later did not differ significantly. The 512 × 512 pixel confocal images were collected with a 63×, 1.2 NA Zeiss C-Apochromat water immersion objective on a Zeiss LSM-410 confocal microscope with ArKr 488-nm laser line for excitation of EGFP. Green emission light was collected between 500 and 530 nm using the standard fluorescein isothiocyanate filter. Immediately after basal image pair (t = 0), direct electrical muscle stimulation was initiated (frequency 2 Hz, duration 60 ms, voltage 1.1–3 V for 3 × 5 min + 1 × 10 min eliciting repeated single contractions). The contractions of the imaged fibers were continually monitored through the oculars of the microscope. Voltage was adjusted accordingly to maintain force. Contraction periods were separated by 90 s of rest. Confocal images were collected at the end of each contraction period. AICAR was given as an intravenous bolus (1 g/kg), and images were collected every 10 min after injection. In the animals given caffeine stimulation, a continuous infusion was given intravenously for 20 min (85 mg/kg) followed by monitoring until 70 min after infusion. The caffeine concentration was modeled after a caffeine concentration (510 mg/kg) previously shown to increase glucose transport in incubated muscle without contractions (29). However, infusing this higher concentration in vivo would result in whole-body contractions, instability, or death of the mouse, thereby interfering with the experiment and imaging.

Image analysis. Images obtained in immunostained muscle fibers were obtained as TIFF images with the Zeiss confocal software and were imported into Metamorph Software (V. 6.1; Universal Imaging Corp., West Chester, PA). Image stacks were created, and maximal and average projections were created. The total number, average gray value intensity, and average area of IL-6 and GM130 vesicular staining were quantified throughout the field of view in the muscle fiber. For the time-lapse image stacks of IL-6-EGFP or EYFP-Golgi, the threshold and the classifying settings of the Metamorph software were adjusted to count the IL-6 vesicles and avoid nonspecific background. Because of variation in the level of IL-6-EGFP or EYFP-Golgi expression between individual transfected fibers, the actual vesicle count divided by the vesicle count at t = 0 (T/T_0) is shown.

Statistical analysis. Vesicle counts obtained from fibers in Metamorph were imported into Sigma plot 10.0 and subjected to paired t test or one way ANOVA against ROI fluorescence values at t = 0 (T/T_0).

RESULTS

IL-6 is located in vesicle-like structures in resting muscle fibers that are reduced by muscle contractions. To determine if mouse TA muscle fibers contain IL-6 protein, we analyzed the intracellular localization of endogenous IL-6 by immuno-staining of intact fixed fibers (Fig. 1). Briefly, mice were anesthetized and the sciatic nerve was attached to electrodes, and the TA muscle in one leg was contracted in situ for 45 min. The contralateral leg was used as a resting, basal control. After contractions, both muscles were excised and fixed. Single muscle fibers were teased from both muscles and immunostained for IL-6. In the TA muscle fibers from the rested leg, IL-6 protein was observed in discrete, dot-like vesicular structures near the sarcolemma (Fig. 1*A*, vertical arrow) and inside the fibers in the area of the T-tubule membranes (Fig. 1*A*, diagonal arrow). The IL-6–positive vesicles were not present in muscle fibers from whole-body IL-6 knockout mice (Fig. 1*C*), demonstrating the specificity of staining. In the TA muscles from the contracted leg, the number of IL-6–positive vesicles within the muscle fibers was significantly reduced (Fig. 1*B*, arrows), which corresponded to a 62% reduction in IL-6 vesicles throughout the muscle fibers (Fig. 1*D*). In order to rule out the possibility that the decrease in IL-6 vesicle number was a result of vesicle fusion, average vesicle

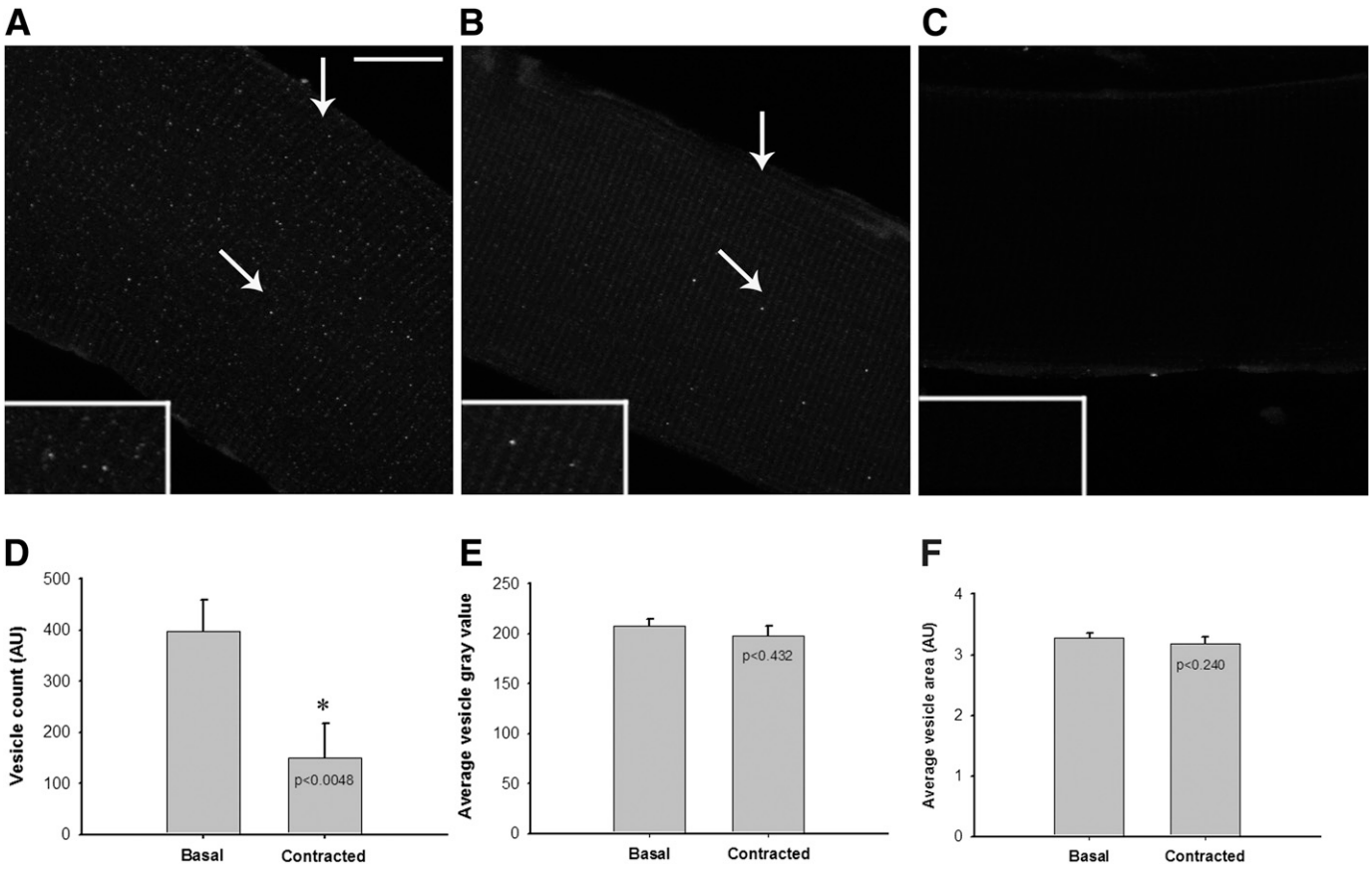

FIG. 1. Endogenous IL-6 is localized in vesicle-like structures in resting muscle fibers, and muscle contraction results in IL-6 vesicle reduction. *A*: Image of IL-6 immunostaining displays IL-6–positive vesicle-like structures (arrows) in a resting TA muscle fiber. Bar = 20 μm. *B*: Image of IL-6 immunostaining in a TA muscle fiber after 45 min of in situ muscle contractions. Similar observations were made in fibers from 6 mice per group. Inserts are magnified parts of the images. *C*: IL-6 knockout TA muscle fibers were immunostained for IL-6 as a negative control. *D*: Image quantification of immunostained IL-6 vesicles from basal and contraction-stimulated muscles, showing a 62% reduction in the number of IL-6–positive vesicles after 45 min of in situ contractions. *E* and *F*: Image quantification of immunostained IL-6 average vesicle light intensity (pixel gray value) (*E*) and mean area (pixel area) (*F*) from basal and contraction-stimulated muscles, showing no changes in the average intensity or size of the IL-6–positive vesicles after 45 min of in situ contractions compared with basal. Values are mean ± SE, $n = 6$. *$P < 0.005$.

intensity (Fig. 1*E*) and average vesicle size (Fig. 1*F*) were quantified. There was no significant difference in IL-6 vesicle intensity or average area. These data demonstrate that IL-6 protein is abundant in vesicular structures inside mouse muscle fibers and that the number of intramyofibril IL-6 vesicles is reduced following muscle contractions.

To ensure that the decrease in IL-6 vesicles was not caused by a general contraction-induced protein leak from the muscle fibers, we stained for an endogenous nonsecreted protein, GM130. GM130 is a widely used marker that is bound to the Golgi membranes helping to maintain the *cis*-Golgi structure (30). Under resting conditions, GM130-positive structures were located in dot-like vesicles throughout the muscle fiber at both the sarcolemma and T-tubule regions (Fig. 2*A*, arrows). The localization, number, intensity, and average area of GM130-positive vesicle structures did not change during 45 min of in situ contractions (Fig. 2*B*, arrows; Fig. 2*C*). Thus, in contrast to IL-6 (Fig. 1), the GM130-positive structures are not reduced during fiber contraction. These data indicate that the contraction-induced reduction in IL-6–positive vesicles is not due to a general protein leak from the muscle fibers (Fig. 2).

Muscle contractions gradually deplete vesicular IL-6 in muscle fibers in vivo. To determine the kinetics of contraction-mediated IL-6 vesicle reduction, we analyzed IL-6 vesicle localization and number in muscle fibers before, during, and after a bout of muscle contractions in situ. We expressed IL-6-EGFP in the superficial portion of the quadriceps muscle in living mice using gene gun transfection (26–28,31–33). Five days later, mice were anesthetized and the transfected fibers were subjected to intravital imaging (34). An image was collected just beneath the sarcolemma surface (fiber surface position) along with another image 6 μm inside the fiber (fiber interior position). During basal conditions, IL-6-EGFP was localized in vesicular structures at the surface position of the transfected muscle fiber (Fig. 3*A*, $t = 0$) and throughout the interior location (Fig. 3*B*, $t = 0$). Thus, IL-6-EGFP–positive vesicles were located similarly to the endogenous IL-6–positive vesicles described in Fig. 1. Immediately after recording the basal ($t = 0$) images, the muscle fibers were subjected to in situ contractions for 3×5 min and 1×10 min, with each contraction bout separated by 90 s of rest. Images were obtained between each contraction bout at both surface (Fig. 3*A*) and interior positions (Fig. 3*B*). The number of IL-6-EGFP vesicles in both positions was reduced by approximately 50% during the first 15 min of contractions (Fig. 3*C*), and the last 10 min of contraction further reduced IL-6-EGFP vesicles to 40% of basal (Fig. 3*C*). The quantitative data are similar to the reduction of endogenous IL-6 found by immunostaining (Fig. 1). To confirm the imaging

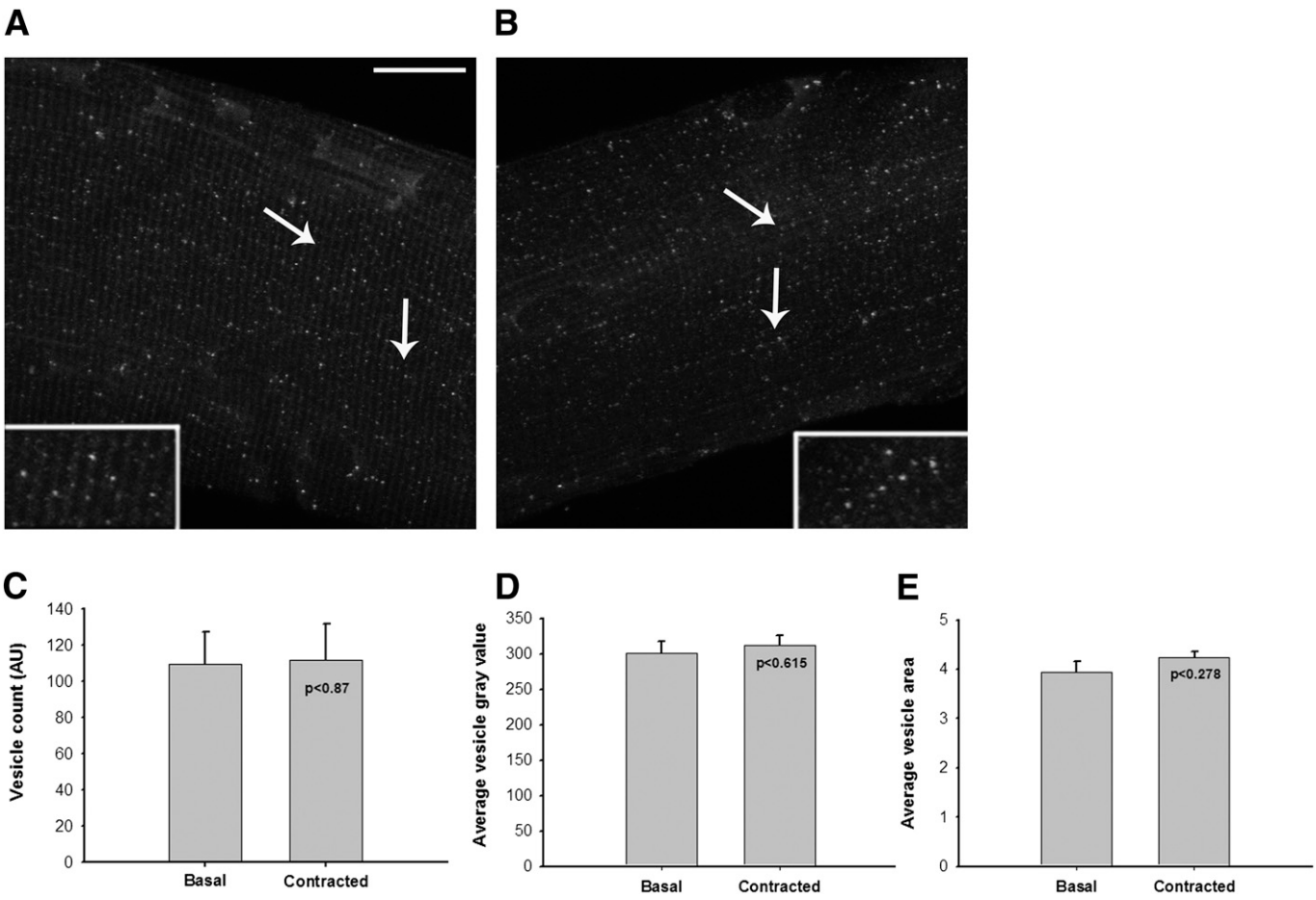

FIG. 2. Endogenous GM130 is localized in vesicle-like structures in resting muscle fibers and is not reduced by muscle contractions. *A*: Image of GM130 immunostaining; shown are GM130-positive structures (arrows) in resting TA muscle fiber. Bar = 20 μm. *B*: Image of GM130 immunostaining in TA muscle fibers subjected to 45 min of in situ muscle contractions. Similar observations were made in fibers from 6 mice. Inserts are magnified parts of the images. Bars = 20 μm. *C–E*: Quantification of immunostained GM130 vesicle number (*C*), average vesicle light intensity (*D*), and average vesicle size (*E*) from basal and contraction-stimulated muscle fibers. No significant reduction in number, intensity, or area of GM130-positive vesicles was detected after 45 min of in situ contractions. Values are mean ± SE, *n* = 6.

results of contraction-mediated IL-6 depletion from single muscle fibers on a whole-muscle level, IL-6-EGFP was expressed in gastrocnemius muscles of NMRI mice using in vivo electroporation. In situ contractions resulted in a 68% reduction in IL-6-EGFP protein (Fig. 3*D*, $P = 0.02$, $n = 3$), comparable to the reduction in vesicle number observed using imaging.

Taken together, these intravital images show that IL-6 is localized to vesicular structures throughout the muscle fibers and that contractions induce a continuous reduction of IL-6 within the muscle fibers over time (Fig. 3).

Similar to the experiments of GM130 immunostaining, we performed in vivo imaging of a fluorescent tagged *trans*-Golgi marker 1,4-galactosyltransferase (35) fused N-terminally to EYFP (EYFP-Golgi). This was done to ensure that the disappearance of IL-6-EGFP was not due to a contraction-induced protein leak from muscle fibers during in vivo contractions. In the basal state, EYFP-Golgi was localized in a dotted vesicular like pattern (Fig. 4*A* and *B*; $t = 0$ in *B*) similar to GM130 (Fig. 2). There was no reduction in EYFP-Golgi after 25 min of in situ contractions (Fig. 4*A–C*; $t = 5–25$ in *B*).

AICAR decreases vesicular IL-6-EGFP–positive vesicles in skeletal muscle. Incubation of intact soleus and extensor digitorum longus muscles in vitro with the AMPK activator AICAR for 2 h has been shown to inhibit IL-6 production (23), whereas AICAR incubation of cultured human myotubes for 24 h increases IL-6 mRNA (21,36). Here, we determined if short term AICAR infusion results in the release of IL-6 from muscle fibers. Quadriceps muscles were transfected with IL-6-EGFP, and 5 days later mice were injected intravenously with a bolus of AICAR (1g/kg). Changes in IL-6-EGFP were measured using time-lapse imaging of IL-6-EGFP in situ. AICAR injection resulted in a gradual decrease in IL-6-EGFP vesicles at both surface (Fig. 5*A*) and interior (Fig. 5*B*) positions of the muscle fibers. The reduction of IL-6-EGFP was specific to AICAR injection, since saline did not result in a significant reduction of IL-6-EGFP (Fig. 5*C* and *D*). The decrease in IL-6-EGFP reached a plateau 70 min after injection, with an approximately 50% reduction in both positions (Fig. 5*C* and *D*). To determine if AMPK activity mediated the effects of AICAR on IL-6, we used muscle-specific transgenic mice that express inactive AMPKα2, the major AMPK catalytic isoform expressed in skeletal muscle. AICAR did not decrease IL-6-EGFP vesicle number in muscle-specific AMPKα2-inactive mice (Fig. 5*E* and *F*). AICAR had no effect on the Golgi marker EYFP-Golgi (Fig. 6*A–D*). These results indicate that AICAR decreases IL-6-EGFP vesicle number in muscle fibers to a degree comparable to that of in situ contractions (Fig. 4) and that AMPKα2 mediates AICAR-stimulated IL-6-EGFP vesicle reduction.

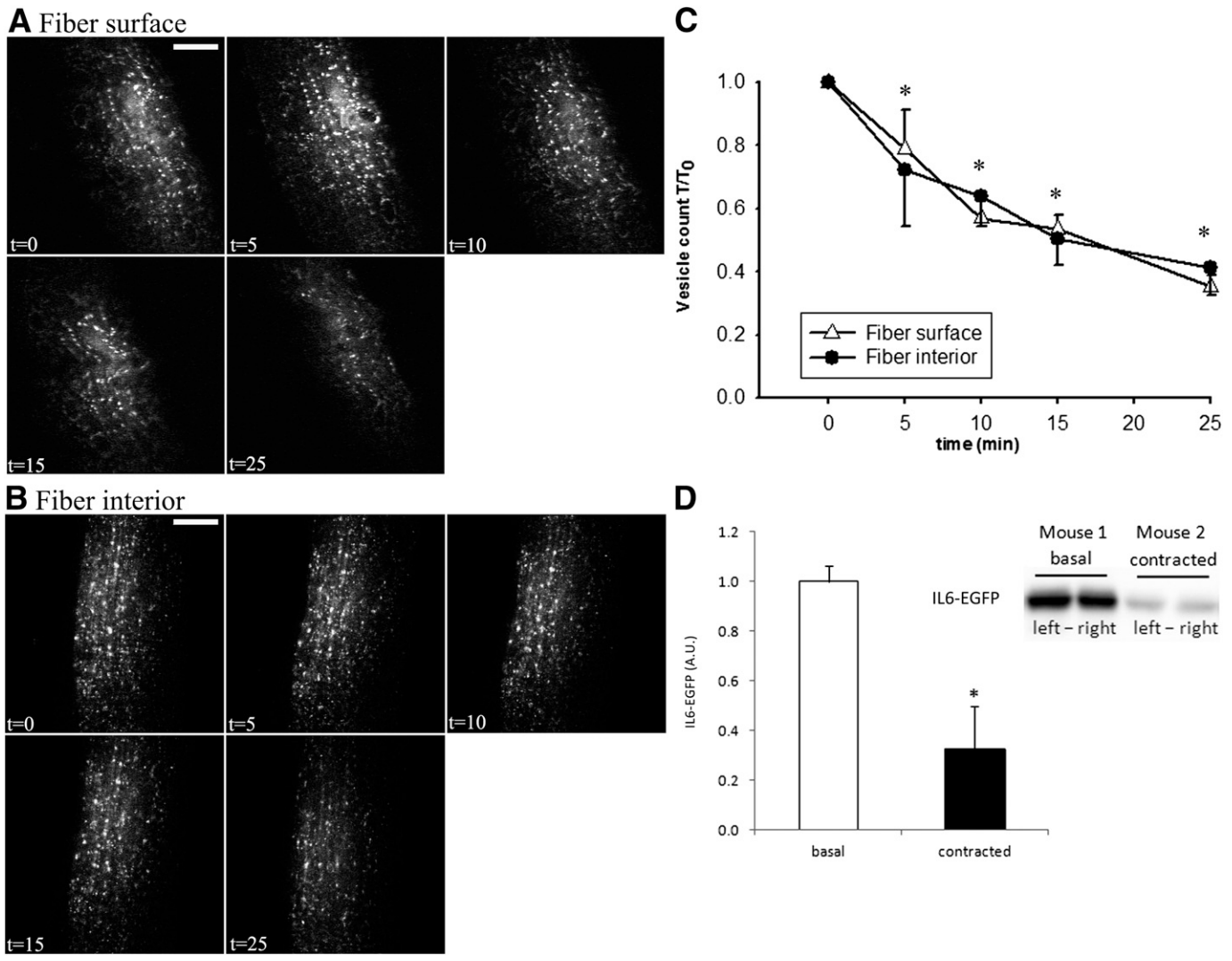

FIG. 3. IL-6-EGFP vesicles are significantly and continuously reduced in mouse muscle fibers during in situ contractions. *A* and *B*: t = 0 confocal images of a basal quadriceps muscle fiber expressing IL-6-EGFP just prior to in situ contractions in a mouse. IL-6-EGFP is localized to vesicle-like structures both near the surface position (*A*) and interior position (6 μm deeper) in the muscle fiber (*B*). In situ contractions were elicited for 3 × 5 min periods (t = 5, 10, 15) and then a 10-min period (t = 25), each separated by 90 s of rest. t = denotes accumulated contraction time. Similar observations were made in fibers from 7 mice. Bar = 20 μm. *C*: Image quantification of IL-6-EGFP vesicle structures from images taken at the surface or interior positions of the muscle fibers following each contraction period. Values are mean ± SE, n = 7. *Denotes significant difference, $P < 0.05$ compared to t = 0. *D*: Western blot of IL-6-EGFP protein reduction in basal or contracted IL-6-EGFP electroporated gastrocnemius muscles. Values are mean ± SE, n = 3 mice. *Denotes significant difference, $P < 0.05$.

Caffeine does not decrease vesicular IL-6 in skeletal muscle. Calcium is essential for excitation-contraction coupling in muscle and is a well-established trigger signal for vesicle reduction in many secretory cell types (37). To determine if calcium mediates IL-6 vesicle reduction, the calcium releasing agent caffeine was infused intravenously from 0–20 min at the highest dose (85 mg/kg) possible without inducing whole-body muscle contractions and larger movements due to the systemic delivery in the living mice. Caffeine had no effect on IL-6-EGFP or Golgi marker EYFP-Golgi vesicles during the 20 min of caffeine infusion or during the 50-min period after infusion (Fig. 7*A*–*C*). In contrast, the caffeine infusion led to significant increases in phosphorylation of Ca^2+/calmodulin-dependent protein kinase II both during and after infusion, indicating that the caffeine infusion protocol had an effect at the cellular level (Fig. 7*E*).

Contraction-stimulated IL-6 vesicle reduction is not mediated by AMPKα2 activity. Our results with AICAR and caffeine led us to hypothesize that AMPK, but not calcium signaling, is important for contraction-mediated IL-6 reduction. Therefore, we used the muscle-specific AMPKα2 inactive transgenic mice to test this hypothesis. Under basal conditions, IL-6-EGFP–positive vesicles were similarly distributed throughout the muscle fibers when comparing control mice with AMPKα2-inactive transgenic mice (Fig. 8*A* and *B*). Muscle contractions similarly reduced IL-6-EGFP vesicles at the surface and interior positions in both wild-type and transgenic mice, demonstrating that the contraction-induced reduction of IL-6 in AMPKα2 inactive transgenic was fully intact (Fig. 8*A* and *B*).

DISCUSSION

Physical exercise is an important modality to improve whole-body metabolic state and insulin sensitivity. It has been postulated that IL-6 secretion from exercising skeletal muscle contributes to the exercise-induced changes

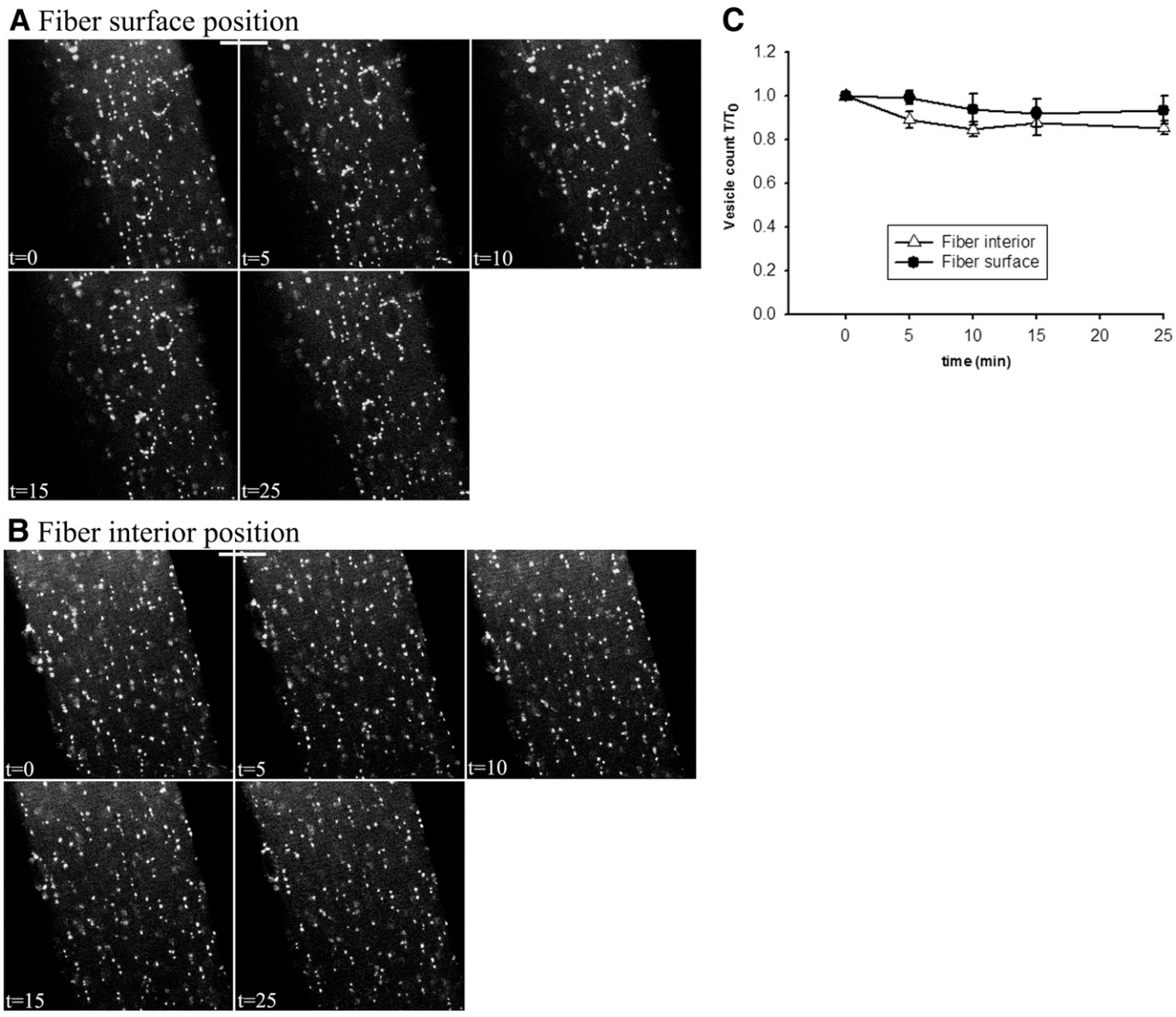

FIG. 4. In situ contraction does not reduce EYFP-Golgi vesicle structure content. *A* and *B*: *t* = 0 shows confocal images of a basal mouse quadriceps muscle fiber expressing EYFP-Golgi just prior to in situ contractions. EYFP-Golgi localized to vesicle-like structures at the surface (*A*) or interior positions (*B*) in a muscle fiber. In situ contractions were elicited for 3 × 5 min periods (*t* = 5, 10, 15) and then a 10-min period (*t* = 25), each separated by 90 s of rest. Similar observations were made in fibers from 7 mice. Bar = 20 μm. *C*: Image quantification of EYFP-Golgi vesicles structure at the surface or interior positions of the muscle fibers following each contraction period. Values are mean ± SE, *n* = 7.

in whole-body metabolism, making IL-6 essential for the beneficial effects of exercise on glucose homeostasis (38). However, data establishing the presence and/or secretion of IL-6 in fully differentiated skeletal muscle has been inconclusive (11–13). Previous studies using lower resolution imaging of sectioned skeletal muscle suggested that under basal conditions there is very little IL-6 protein expression within the muscle fibers (11–13). Here, we imaged single intact fixed muscle fibers or living muscle fibers at high resolution and detected significant amounts of intracellular IL-6–positive vesicles under resting conditions at both the sarcolemma and T-tubule regions. The vesicles were specific for IL-6, as these vesicles were not present in the muscle fibers of IL-6 knockout mice. Thus, these data clearly establish that IL-6 is present within skeletal muscle fibers.

Muscle contraction and AICAR stimulation reduced IL-6–positive vesicles from both surface and interior positions within living muscle fibers. Because muscle fibers have a T-tubule network that plays a central role in transmembrane substrate and hormone exchange with serum (27,31,39), the localization of IL-6 inside the muscle fiber in the vicinity of the T-tubule membranes is logical, since this would increase the surface area available for efficient release of IL-6. Consistent with this hypothesis, contraction-induced IL-6 vesicle reduction was rapid, with a significant decrease in IL-6 vesicles occurring after only 5 min of muscle contractions. Our findings are compatible with a secretory function of muscle fibers and demonstrate that skeletal muscle fibers function as classic endocrine cells containing depots of IL-6–positive intracellular vesicles that are reduced upon contraction stimulation. The concept of skeletal muscle fibers as a secretory cell is also

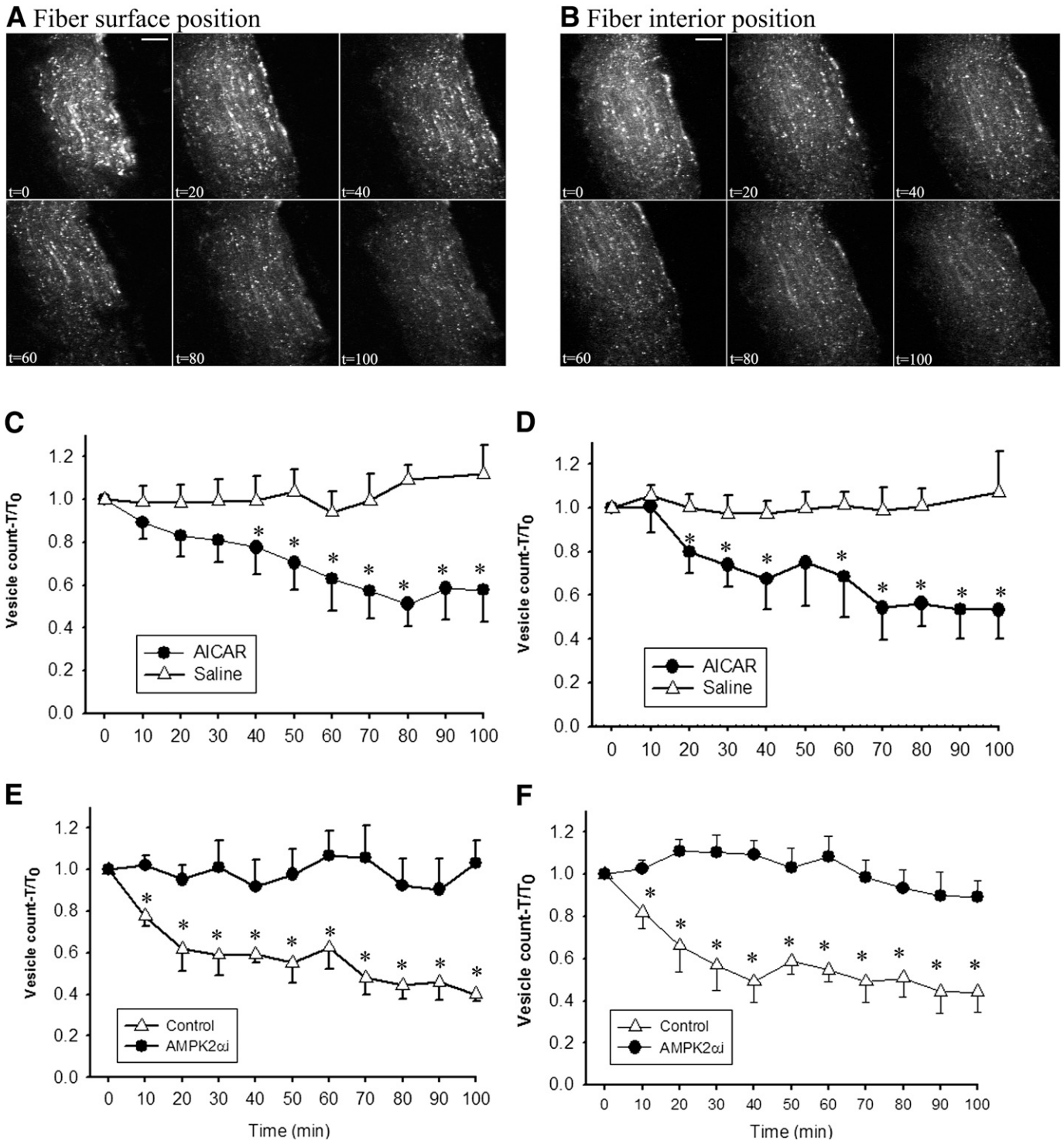

FIG. 5. IL-6-EGFP vesicles are gradually and significantly reduced by AICAR stimulation. *A* and *B*: $t = 0$ shows confocal images of basal IL-6-EGFP vesicles at the surface (*A*) or interior (*B*) positions in a mouse quadriceps muscle fiber prior to i.v. administration of an AICAR bolus. Immediately after $t = 0$, the AICAR bolus was given via tail vein. Similar observations were made in fibers from 5–6 mice. t = denotes accumulated time after the bolus injection. Bar = 20 μm. *C* and *D*: Image quantification of IL-6-EGFP vesicles from images taken at the surface position (*C*) or interior position (*D*) throughout the time period after either an AICAR or a saline bolus injection. *E* and *F*: Image quantification of IL-6-EGFP vesicles from images taken at the surface (*C*) or interior (*D*) positions of the muscle fibers in AMPKα2-inactive transgenic mice and wild-type control mice after bolus administration of AICAR. Values are mean ± SE, $n = 5–6$. *$P < 0.05$ compared with $t = 0$.

supported by data showing that muscles express vesicle-associated membrane protein family members localized to GLUT4 vesicles, and these vesicles are involved in regulated secretion (40). Although the current study presents many lines of evidence that IL-6 vesicles are undergoing stimuli depletion from muscle fibers, consistent with a release of IL-6 into serum, our imaging method cannot visually show a release of IL-6. However, all of the data support that this is the case. In addition to the IL-6 imaging data, we have also shown that the Golgi marker is not

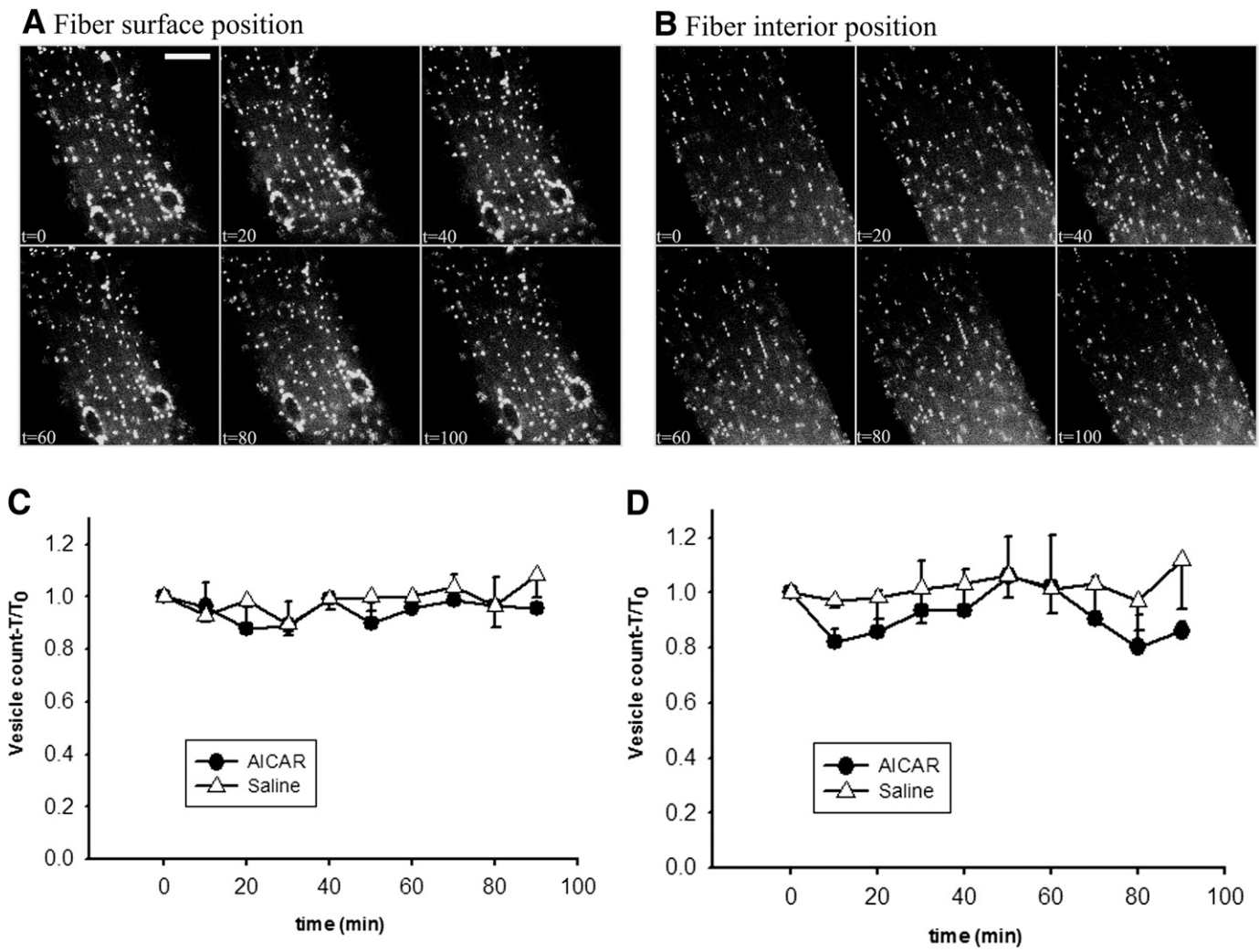

FIG. 6. AICAR or saline stimulation does not reduce vesicle abundance. *A* and *B*: *t* = 0 shows confocal images of basal EYFP-Golgi vesicle structures at the surface (*A*) or interior (*B*) positions in a mouse quadriceps fiber prior to intravenous administration of an AICAR bolus. Similar observations were made in fibers from 5–6 mice. Bar = 20 μm. *C* and *D*: Image quantification of EYFP-Golgi vesicles from images taken at the surface position (*C*) or interior position (*D*) throughout the time period after either an AICAR or a saline bolus injection. Values are mean ± SE, *n* = 5–6.

degraded with any of the stimulation protocols, making it unlikely that IL-6 undergoes nonspecific degradation or leakage. Furthermore, our findings that certain stimuli don't decrease IL-6 vesicle number (AICAR in AMPKα2-inactive transgenic mice, caffeine) also suggest that IL-6 vesicle reduction is specific and not the result of a general, stimuli-induced degradation.

We found that the maximal degree of reduction in number of IL-6 vesicles in the muscle fibers was ~60%, regardless of the intensity and length of the contraction protocol. In contrast, the Golgi marker did not change with any of the protocols. IL-6 vesicle reduction was found without a change in IL-6 vesicle intensity or average area and was confirmed by a similar reduction in IL-6-EGFP protein, indicating that vesicle fusion or redistribution is not the cause of a reduced IL-6 signal. The maximal decrease with AICAR stimulation was similar, with a 50% reduction of IL-6 vesicle content. Interestingly, we have previously reported that muscle contraction results in a maximal reduction in GLUT4 vesicle depots of approximately 70% (34), comparable to maximal IL-6 reduction. These findings suggest there is a limit to the degree of decrease in protein-containing vesicles in skeletal muscle fibers in the order of approximately 60–70%. A maximal limit for secretory vesicle reduction has been described in other cell types such as insulin-secreting pancreatic cells (5–30%) (41), neuroendocrine cells (25%) (42), growth hormone–secreting cells (5–25%) (43), mast cells (30–40%) (44), and chromaffin cells (30%) (45). Lower maximal values for other cell types suggest that the secretory function of muscle may be higher. The higher capacity in muscle may enable protein secretion even under conditions where a low number of muscle fibers or mass of muscles are contracting. This would allow for secretory functions such as myokine secretion or GLUT4 vesicle movement to occur even under conditions such as low-intensity exercise.

Even though our data showing a contraction-mediated IL-6 vesicle reduction is in line with the classical concept of secretory cell kinetics, our findings are in contrast to a study analyzing muscle IL-6 before and after exercise (11). Using immunohistochemistry of muscle sections from human biopsies, it was reported that IL-6, localized primarily in the sarcolemma region, was increased 2 h after bicycle exercise (11). The discrepancy with our data, which revealed

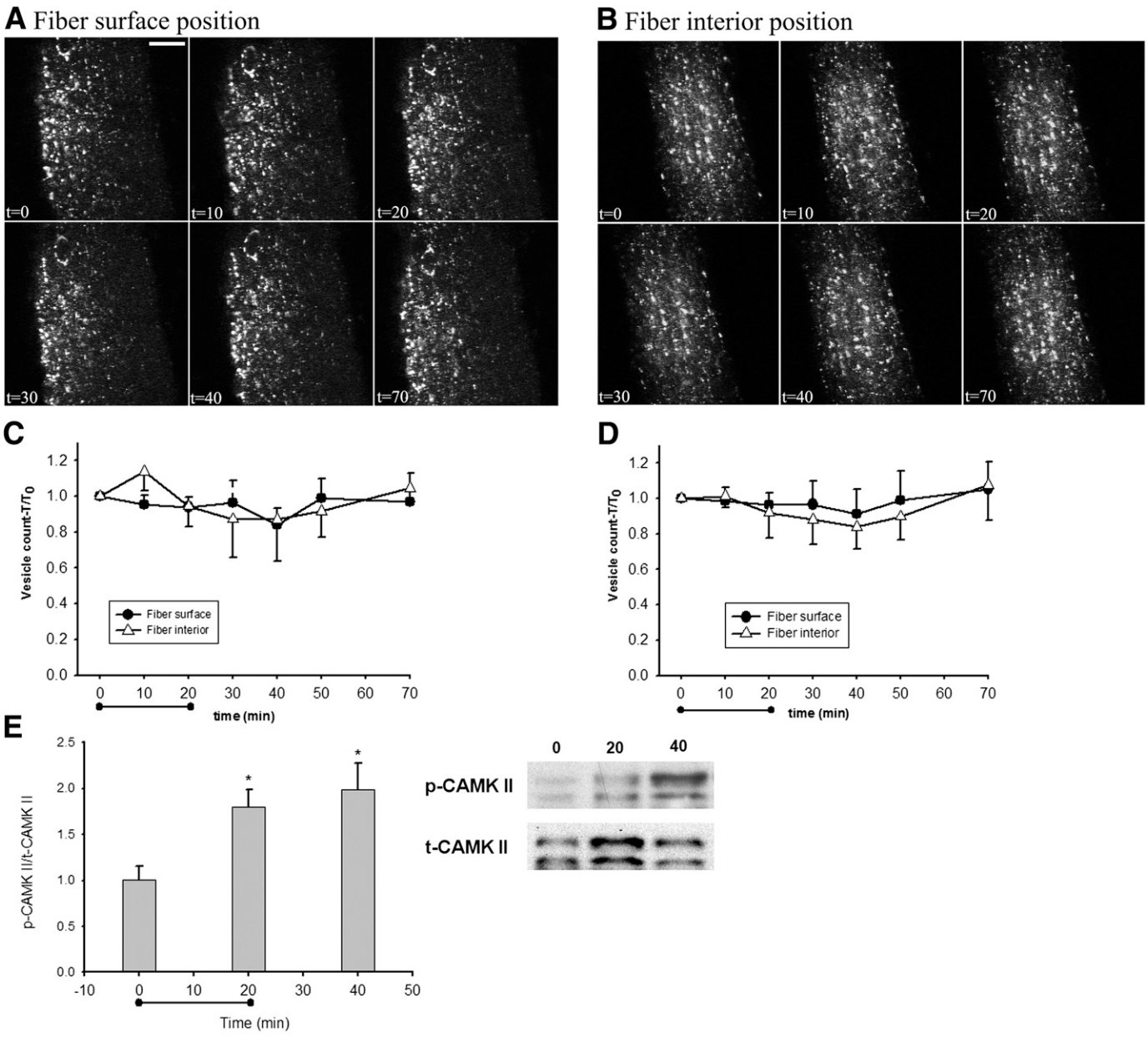

FIG. 7. Caffeine-mediated Ca^2+/calmodulin-dependent protein kinase II (CAMK II) phosphorylation does not reduce IL-6-EGFP or EYFP-Golgi vesicle abundance. *A* and *B*: *t* = 0 shows confocal images of basal IL-6-EGFP vesicles in the surface (*A*) or interior (*B*) part positions of a mouse quadriceps muscle fiber prior to intravenous caffeine infusion. Similar observations were made in fibers from six mice. Bar = 20 μm. Immediately after *t* = 0, caffeine infusion was initiated for 20 min and confocal images were collected every 10 min during and after infusion. *C* and *D*: Image quantification of IL-6-EGFP (*C*) or EYFP-Golgi (*D*) vesicles from images taken at the surface position or interior position throughout the time period after i.v. infusion of caffeine. Values are mean ± SE, *n* = 6. *E*: Western blot of phosphorylated Ca^2+/calmodulin-dependent protein kinase II from muscle either basal, 20, or 40 min after caffeine infusion. Values are mean ± SE, *n* = 5–6. **P* < 0.05.

a decrease in IL-6 signal, could be due to differences in methods because the previous study was based on muscle biopsies and not intact muscle in vivo (11). Interestingly, mouse plantaris muscles subjected to surgical injury showed significant IL-6 protein in the sarcolemma region (10), and it has also been reported that the main source of IL-6 within the muscle in response to muscle biopsy or muscle isolation may be from circulating monocytes such as macrophages (14). Thus, the increase in IL-6 protein observed in the human muscle biopsies after exercise could result from the surgical procedure combined with increased macrophage migration during the exercise bout. Furthermore, an increase in IL-6 protein in the muscle fibers simultaneous with an increase in the circulation is not consistent with classical protein secretion consisting of a net reduction of secretory content from the endocrine cell.

The similarities between our findings with muscle fibers and classical endocrine cells led us to investigate a potential role for calcium in IL-6 vesicle reduction. Although intracellular calcium release is a well-established signal for release of vesicles in secretory cells, we found that caffeine infusion, which resulted in a significant increase in intracellular Ca^2+/calmodulin-dependent protein kinase II phosphorylation, had no effect on IL-6 vesicle distribution. Our results are in line with a recent study in incubated mouse muscles showing that calcium release

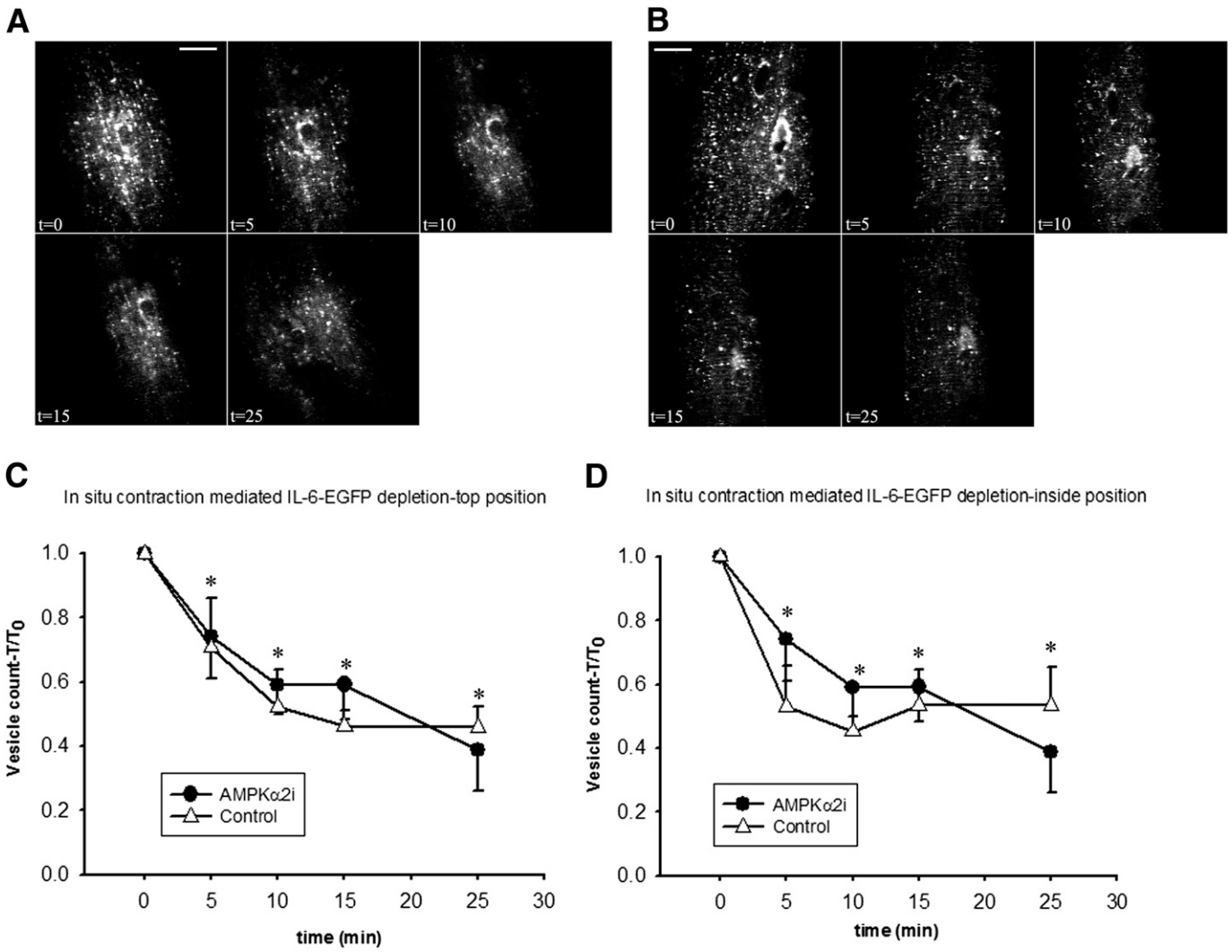

FIG. 8. AMPK activation is not essential for IL-6-EGFP vesicle reduction. *A* and *B*: $t = 0$ shows confocal images of basal quadriceps muscle fibers expressing IL-6-EGFP prior to in situ contractions from either a wild-type control (*A*) or an AMPKα2-inactive transgenic (*B*) mouse. IL-6-EGFP is localized to vesicle-like structures near the surface position in the muscle fibers. The interior positions are not shown but demonstrate similar vesicle distribution. In situ contractions were elicited for 3 × 5 min periods ($t = 5, 10, 15$) and then a 10-min period ($t = 25$), each separated by 90 s of rest. Similar observations were made in fibers from 5–6 mice. Bar = 20 μm. *C* and *D*: Image quantification of IL-6-EGFP vesicles from images taken at the surface (*C*) or interior (*D*) positions of the muscle fibers in AMPKα-inactive transgenic mice and wild-type control mice following each contraction period. Values are mean ± SE, $n = 5–6$. *$P < 0.05$ compared with $t = 0$.

had no effect on IL-6 mRNA production (23). The lack of regulation by calcium is plausible given that even single twitches result in the release of calcium within the myofibers, making discriminate regulation of IL-6 release impossible. Thus, it is likely that calcium signaling does not function in the regulation of IL-6 vesicle reduction in skeletal muscle.

AMPK activation has been hypothesized to regulate, in whole or in part, many of the metabolic and transcriptional responses to exercise, including GLUT4 translocation and glucose transport (46), fatty acid oxidation (47,48), mitochondrial biogenesis (49–51), expression of peroxisome proliferator–activated receptor γ coactivator-1α (51), and fiber type transformation (52). AMPK has also been proposed to be involved in contraction-stimulated IL-6 expression and secretion (19). Bicycle exercise for 60 min was shown to increase both AMPK activity in muscle and IL-6 in serum (19); however, whether AMPK mediates IL-6 vesicle reduction has not been directly tested. Our current finding, that AICAR injection decreases IL-6 vesicles in an AMPKα2-dependent manner, along with our previous work showing that this same AICAR treatment also causes AMPK activation (53), is consistent with the hypothesis that AMPK signaling induces IL-6 vesicle reduction in skeletal muscle. However, the normal contraction-stimulated IL-6 vesicle reduction is intact in AMPKα2-inactive mice. Thus, these results clearly show that AMPKα2 activity is not essential for contraction-stimulated IL-6 reduction. This result is similar to studies in which contraction-mediated glucose transport (24,54,55), GLUT4 translocation (34), and fatty acid oxidation (56) are still intact in animal models of reduced AMPK activity (18). Thus, redundant signaling pathways may also exist for the regulation of IL-6 vesicle reduction with muscle contractions.

In conclusion, we have developed a novel image-based system to analyze the kinetics of vesicular-containing proteins in living skeletal muscle. As new myokines are proposed and their function in metabolic and tissue homeostasis

emerges, this methodology will provide a valuable tool to determine the intracellular source and depletion kinetics of these putative myokines. This study provides the first data that clearly demonstrate that intact muscle fibers act as endocrine cells in response to muscle contractions in vivo by rapid, stimuli-dependent decreases in the secretory vesicle content.

ACKNOWLEDGMENTS

This project was supported by the National Institutes of Health (NIH) grants R01AR45670 and R01DK68626 (L.J.G.) and the DERC P30DK036836 at the Joslin Diabetes Center. H.P.M.M.L. was supported by the Weimann Foundation, the Beckett Foundation, and the Danish National Research Foundation. J.B. was supported by an NIH Training grant (T32-DK-07260-29) and a Gettysburg College Professional Development grant. J.T.T. was supported by the Novo Nordisk Foundation Center for Basic Metabolic Research. No other potential conflicts of interest relevant to this article were reported.

H.P.M.M.L. designed and performed experiments and wrote the manuscript. J.B. designed and performed experiments and edited the manuscript. P.S. constructed the IL-6-EGFP plasmid and reviewed and edited the manuscript. H.-J.K. performed experiments. H.G. contributed to discussion and reviewed and edited the manuscript. M.F.H. and J.T.T. contributed to the experiments. L.J.G. designed experiments and wrote and edited the manuscript. L.J.G. is the guarantor of this work and, as such, had full access to all the data in the study and takes responsibility for the integrity of the data and the accuracy of the data analysis.

REFERENCES

1. Steensberg A, van Hall G, Osada T, Sacchetti M, Saltin B, Klarlund Pedersen B. Production of interleukin-6 in contracting human skeletal muscles can account for the exercise-induced increase in plasma interleukin-6. J Physiol 2000;529:237–242
2. Ouchi N, Oshima Y, Ohashi K, et al. Follistatin-like 1, a secreted muscle protein, promotes endothelial cell function and revascularization in ischemic tissue through a nitric-oxide synthase-dependent mechanism. J Biol Chem 2008;283:32802–32811
3. Izumiya Y, Bina HA, Ouchi N, Akasaki Y, Kharitonenkov A, Walsh K. FGF21 is an Akt-regulated myokine. FEBS Lett 2008;582:3805–3810
4. Zeng L, Akasaki Y, Sato K, Ouchi N, Izumiya Y, Walsh K. Insulin-like 6 is induced by muscle injury and functions as a regenerative factor. J Biol Chem 2010;285:36060–36069
5. Boström P, Wu J, Jedrychowski MP, et al. A PGC1-α-dependent myokine that drives brown-fat-like development of white fat and thermogenesis. Nature 2012;481:463–468
6. Steensberg A, Keller C, Starkie RL, Osada T, Febbraio MA, Pedersen BK. IL-6 and TNF-alpha expression in, and release from, contracting human skeletal muscle. Am J Physiol Endocrinol Metab 2002;283:E1272–E1278
7. Carey AL, Steinberg GR, Macaulay SL, et al. Interleukin-6 increases insulin-stimulated glucose disposal in humans and glucose uptake and fatty acid oxidation in vitro via AMP-activated protein kinase. Diabetes 2006;55:2688–2697
8. Keller C, Steensberg A, Pilegaard H, et al. Transcriptional activation of the IL-6 gene in human contracting skeletal muscle: influence of muscle glycogen content. FASEB J 2001;15:2748–2750
9. Brandt C, Jakobsen AH, Adser H, et al. IL-6 regulates exercise and training-induced adaptations in subcutaneous adipose tissue in mice. Acta Physiol (Oxf) 2012;205:224–235
10. Serrano AL, Baeza-Raja B, Perdiguero E, Jardí M, Muñoz-Cánoves P. Interleukin-6 is an essential regulator of satellite cell-mediated skeletal muscle hypertrophy. Cell Metab 2008;7:33–44
11. Hiscock N, Chan MH, Bisucci T, Darby IA, Febbraio MA. Skeletal myocytes are a source of interleukin-6 mRNA expression and protein release during contraction: evidence of fiber type specificity. FASEB J 2004;18:992–994
12. Garibotto G, Sofia A, Procopio V, et al. Peripheral tissue release of interleukin-6 in patients with chronic kidney diseases: effects of end-stage renal disease and microinflammatory state. Kidney Int 2006;70:384–390
13. Raj DS, Dominic EA, Pai A, et al. Skeletal muscle, cytokines, and oxidative stress in end-stage renal disease. Kidney Int 2005;68:2338–2344
14. Schiøtz Thorud HM, Wisløff U, Lunde PK, Christensen G, Ellingsen O, Sejersted OM. Surgical manipulation, but not moderate exercise, is associated with increased cytokine mRNA expression in the rat soleus muscle. Acta Physiol Scand 2002;175:219–226
15. Steensberg A, Fischer CP, Sacchetti M, et al. Acute interleukin-6 administration does not impair muscle glucose uptake or whole-body glucose disposal in healthy humans. J Physiol 2003;548:631–638
16. Febbraio MA, Steensberg A, Keller C, et al. Glucose ingestion attenuates interleukin-6 release from contracting skeletal muscle in humans. J Physiol 2003;549:607–612
17. Febbraio MA, Ott P, Nielsen HB, et al. Hepatosplanchnic clearance of interleukin-6 in humans during exercise. Am J Physiol Endocrinol Metab 2003;285:E397–E402
18. Fujii N, Jessen N, Goodyear LJ. AMP-activated protein kinase and the regulation of glucose transport. Am J Physiol Endocrinol Metab 2006;291:E867–E877
19. MacDonald C, Wojtaszewski JF, Pedersen BK, Kiens B, Richter EA. Interleukin-6 release from human skeletal muscle during exercise: relation to AMPK activity. J Appl Physiol 2003;95:2273–2277
20. Steensberg A, Toft AD, Schjerling P, Halkjaer-Kristensen J, Pedersen BK. Plasma interleukin-6 during strenuous exercise: role of epinephrine. Am J Physiol Cell Physiol 2001;281:C1001–C1004
21. Weigert C, Düfer M, Simon P, et al. Upregulation of IL-6 mRNA by IL-6 in skeletal muscle cells: role of IL-6 mRNA stabilization and Ca^2+-dependent mechanisms. Am J Physiol Cell Physiol 2007;293:C1139–C1147
22. Lihn AS, Pedersen SB, Lund S, Richelsen B. The anti-diabetic AMPK activator AICAR reduces IL-6 and IL-8 in human adipose tissue and skeletal muscle cells. Mol Cell Endocrinol 2008;292:36–41
23. Glund S, Treebak JT, Long YC, et al. Role of adenosine 5′-monophosphate-activated protein kinase in interleukin-6 release from isolated mouse skeletal muscle. Endocrinology 2009;150:600–606
24. Fujii N, Hirshman MF, Kane EM, et al. AMP-activated protein kinase alpha2 activity is not essential for contraction- and hyperosmolarity-induced glucose transport in skeletal muscle. J Biol Chem 2005;280:39033–39041
25. Ploug T, van Deurs B, Ai H, Cushman SW, Ralston E. Analysis of GLUT4 distribution in whole skeletal muscle fibers: identification of distinct storage compartments that are recruited by insulin and muscle contractions. J Cell Biol 1998;142:1429–1446
26. Lauritzen HPMM, Reynet C, Schjerling P, et al. Gene gun bombardment-mediated expression and translocation of EGFP-tagged GLUT4 in skeletal muscle fibers in vivo. Pflugers Arch 2002;444:710–721
27. Lauritzen HP, Ploug T, Prats C, Tavaré JM, Galbo H. Imaging of insulin signaling in skeletal muscle of living mice shows major role of T-tubules. Diabetes 2006;55:1300–1306
28. Lauritzen HP, Galbo H, Brandauer J, Goodyear LJ, Ploug T. Large GLUT4 vesicles are stationary while locally and reversibly depleted during transient insulin stimulation of skeletal muscle of living mice: imaging analysis of GLUT4-enhanced green fluorescent protein vesicle dynamics. Diabetes 2008;57:315–324
29. YOUN JH, Gulve EA, Holloszy JO. Calcium stimulates glucose transport in skeletal muscle by a pathway independent of contraction. Am J Physiol 1991;260(3 Pt 1):C555–C561
30. Nakamura N, Rabouille C, Watson R, et al. Characterization of a cis-Golgi matrix protein, GM130. J Cell Biol 1995;131:1715–1726
31. Lauritzen HP, Ploug T, Ai H, Donsmark M, Prats C, Galbo H. Denervation and high-fat diet reduce insulin signaling in T-tubules in skeletal muscle of living mice. Diabetes 2008;57:13–23
32. Lauritzen HP. Imaging of protein translocation in situ in skeletal muscle of living mice. Methods Mol Biol 2010;637:231–244
33. Lauritzen HP, Schertzer JD. Measuring GLUT4 translocation in mature muscle fibers. Am J Physiol Endocrinol Metab 2010;299:E169–E179
34. Lauritzen HP, Galbo H, Toyoda T, Goodyear LJ. Kinetics of contraction-induced GLUT4 translocation in skeletal muscle fibers from living mice. Diabetes 2010;59:2134–2144
35. Henneberry AL, Wright MM, McMaster CR. The major sites of cellular phospholipid synthesis and molecular determinants of Fatty Acid and lipid head group specificity. Mol Biol Cell 2002;13:3148–3161
36. Du JH, Xu N, Song Y, et al. AICAR stimulates IL-6 production via p38 MAPK in cardiac fibroblasts in adult mice: a possible role for AMPK. Biochem Biophys Res Commun 2005;337:1139–1144

37. Pang ZP, Südhof TC. Cell biology of Ca^2+-triggered exocytosis. Curr Opin Cell Biol 2010;22:496–505
38. Pedersen BK. Edward F. Adolph distinguished lecture: muscle as an endocrine organ: IL-6 and other myokines. J Appl Physiol 2009;107:1006–1014
39. Wang W, Hansen PA, Marshall BA, Holloszy JO, Mueckler M. Insulin unmasks a COOH-terminal Glut4 epitope and increases glucose transport across T-tubules in skeletal muscle. J Cell Biol 1996;135:415–430
40. Rose AJ, Jeppesen J, Kiens B, Richter EA. Effects of contraction on localization of GLUT4 and v-SNARE isoforms in rat skeletal muscle. Am J Physiol Regul Integr Comp Physiol 2009;297:R1228–R1237
41. Straub SG, Shanmugam G, Sharp GW. Stimulation of insulin release by glucose is associated with an increase in the number of docked granules in the beta-cells of rat pancreatic islets. Diabetes 2004;53:3179–3183
42. Dixon WR, Garcia AG, Kirpekar SM. Release of catecholamines and dopamine beta-hydroxylase from the perfused adrenal gland of the cat. J Physiol 1975;244:805–824
43. Ohara-Imaizumi M, Aoyagi K, Akimoto Y, et al. Imaging exocytosis of single glucagon-like peptide-1 containing granules in a murine enteroendocrine cell line with total internal reflection fluorescent microscopy. Biochem Biophys Res Commun 2009;390:16–20
44. García-Faroldi G, Rodríguez CE, Urdiales JL, et al. Polyamines are present in mast cell secretory granules and are important for granule homeostasis. PLoS ONE 2010;5:e15071
45. Montesinos MS, Machado JD, Camacho M, et al. The crucial role of chromogranins in storage and exocytosis revealed using chromaffin cells from chromogranin A null mouse. J Neurosci 2008;28:3350–3358
46. O'Neill HM, Maarbjerg SJ, Crane JD, et al. AMP-activated protein kinase (AMPK) beta1beta2 muscle null mice reveal an essential role for AMPK in maintaining mitochondrial content and glucose uptake during exercise. Proc Natl Acad Sci USA 2011;108:16092–16097
47. Merrill GF, Kurth EJ, Hardie DG, Winder WW. AICA riboside increases AMP-activated protein kinase, fatty acid oxidation, and glucose uptake in rat muscle. Am J Physiol 1997;273:E1107–E1112
48. Thomson DM, Brown JD, Fillmore N, et al. LKB1 and the regulation of malonyl-CoA and fatty acid oxidation in muscle. Am J Physiol Endocrinol Metab 2007;293:E1572–E1579
49. Zong H, Ren JM, Young LH, et al. AMP kinase is required for mitochondrial biogenesis in skeletal muscle in response to chronic energy deprivation. Proc Natl Acad Sci USA 2002;99:15983–15987
50. Reznick RM, Zong H, Li J, et al. Aging-associated reductions in AMP-activated protein kinase activity and mitochondrial biogenesis. Cell Metab 2007;5:151–156
51. Jäger S, Handschin C, St-Pierre J, Spiegelman BM. AMP-activated protein kinase (AMPK) action in skeletal muscle via direct phosphorylation of PGC-1alpha. Proc Natl Acad Sci USA 2007;104:12017–12022
52. Röckl KS, Hirshman MF, Brandauer J, Fujii N, Witters LA, Goodyear LJ. Skeletal muscle adaptation to exercise training: AMP-activated protein kinase mediates muscle fiber type shift. Diabetes 2007;56:2062–2069
53. Fujii N, Seifert MM, Kane EM, et al. Role of AMP-activated protein kinase in exercise capacity, whole body glucose homeostasis, and glucose transport in skeletal muscle -insight from analysis of a transgenic mouse model-. Diabetes Res Clin Pract 2007;77(Suppl. 1):S92–S98
54. Maarbjerg SJ, Jørgensen SB, Rose AJ, et al. Genetic impairment of AMPK-alpha2 signaling does not reduce muscle glucose uptake during treadmill exercise in mice. Am J Physiol Endocrinol Metab 2009;297:E924–E934
55. Jørgensen SB, Viollet B, Andreelli F, et al. Knockout of the alpha2 but not alpha1 5′-AMP-activated protein kinase isoform abolishes 5-aminoimidazole-4-carboxamide-1-beta-4-ribofuranosidebut not contraction-induced glucose uptake in skeletal muscle. J Biol Chem 2004;279:1070–1079
56. Dzamko N, Schertzer JD, Ryall JG, et al. AMPK-independent pathways regulate skeletal muscle fatty acid oxidation. J Physiol 2008;586:5819–5831